Research Papers

GREENSUSMATER

Greensusmater
Vol. 2, No. 1, 2025
https://doi.org/10.62755/greensusmater.2025.2.1.21-29

Check for updates

Synthesis and Characterization of Electrospun Edible Bird's Nest/Polyvinylpyrrolidone Nanofibers

Dian Ahmad Hapidin[2], Aan Priyanto[1,2], Eka Sentia Ayu Listari[2], Dhewa Edikresnha[2], Khairurrijal Khairurrijal[2,3]

[1] *Doctoral Program of Physics, Faculty of Mathematics and Natural Sciences, Institut Teknologi Bandung, Jalan Ganesa 10, Bandung 40132, Indonesia*
[2] *Department of Physics, Faculty of Mathematics and Natural Sciences, Institut Teknologi Bandung, Jalan Ganesa 10, Bandung 40132, Indonesia*
[3] *University Center of Excellence – Nutraceutical, Bioscience and Biotechnology Research Center, Institut Teknologi Bandung, Jalan Ganesa 10, Bandung 40132, Indonesia*

Corresponding author: dian.ahmad@itb.ac.id

ARTICLE HISTORY: Received: June 16, 2025 | Revised: June 16, 2025 | Accepted: June 30, 2025

ABSTRACT

Edible Bird's nest (EBN) is a highly valuable food product due to its rich nutritional content and potential health benefits. In this study, we investigated the morphology and diameter of electrospun EBN/PVP nanofibers by exploring different solution and electrospinning parameters. Smooth, homogeneous, and defect-free nanofibers were obtained using EBN:PVP ratios ranging from 10:90 to 60:40. Increasing the concentration of EBN in the solution resulted in fibers with larger diameters. The fiber diameter was found to decrease with increasing voltage of the electrospinning process. In addition, increasing the needle-to-collector distance resulted in fibers with smaller diameters. The FTIR spectrum of EBN/PVP showed a combination of the spectral characteristics of both components. The EBN/PVP nanofiber blend showed improved thermal stability, probably due to the interaction between EBN and PVP, which strengthened the blend structure. EBN/PVP nanofibers with dominant EBN content can be very useful as a matrix to protect bioactive ingredients from environmental degradation while allowing controlled release.

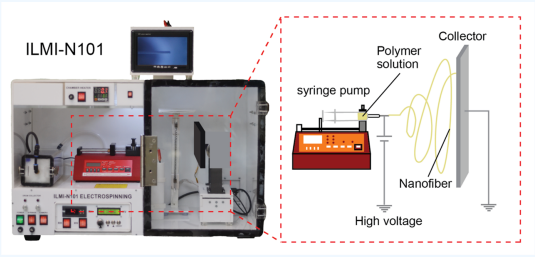

Keywords: *Edible bird's nest, Electrospinning, Nanofiber, Polyvinylpyrrolidone*

1. INTRODUCTION

Edible Bird's Nest (EBN) is a secretion produced by swiftlets that has been known and used as a functional food and natural medicine [1, 2]. EBN has gained popularity for making various dietary supplements such as capsules, drinks and snacks [3, 4]. EBN produced from hardened swiftlet saliva is rich in nutrients such as protein, essential amino acids, and various minerals, making it a potential material for the development of health and wellness products [5, 6, 7]. EBN has interesting potential to be used as a matrix in the form of nanofibers, especially because of its rich nutritional content, biocompatibility, bioactive properties, and multifunctional applications [5, 7, 8, 9].

Electrospun nanofibers from pure EBN may not be possible due to the glycoprotein content, which provides bioactive and nutritional properties. These glycoproteins often have low solubility in common solvents, making it difficult for the electrospinning process to produce nanofibers from pure EBN [10]. To overcome the solubility problem, EBN often needs to be mixed with other polymers. One of the polymers often used in composites with bioactive materials is polyvinylpyrrolidone (PVP) [11]. PVP is a biocompatible and water soluble polymer commonly used in electrospinning [12, 13]. The use of PVP as a carrier material for EBN can increase the solubility of EBN in solvents and promote the formation of uniform and stable nanofibers during electrospinning, thus producing nanofibers with higher EBN content.

Nanofibers can be synthesized by several methods, such as self-assembly [14], phase separation [15], lyophilization [16] and electrospinning [17]. However, the electrospinning technique is the most popular method for fabricating nanofibers due to its ability to produce fibers with very small diameters and good control over morphology [18].

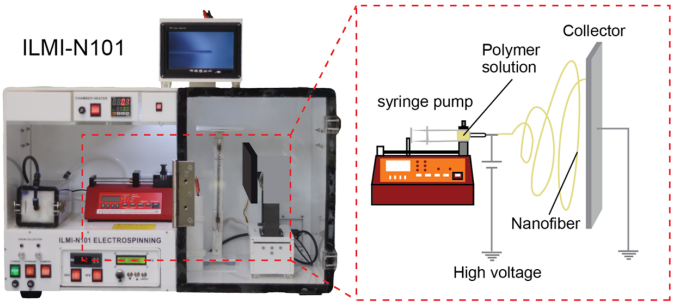

Figure 1. ILMI-N101 electrospinning device and it's schematic illustration

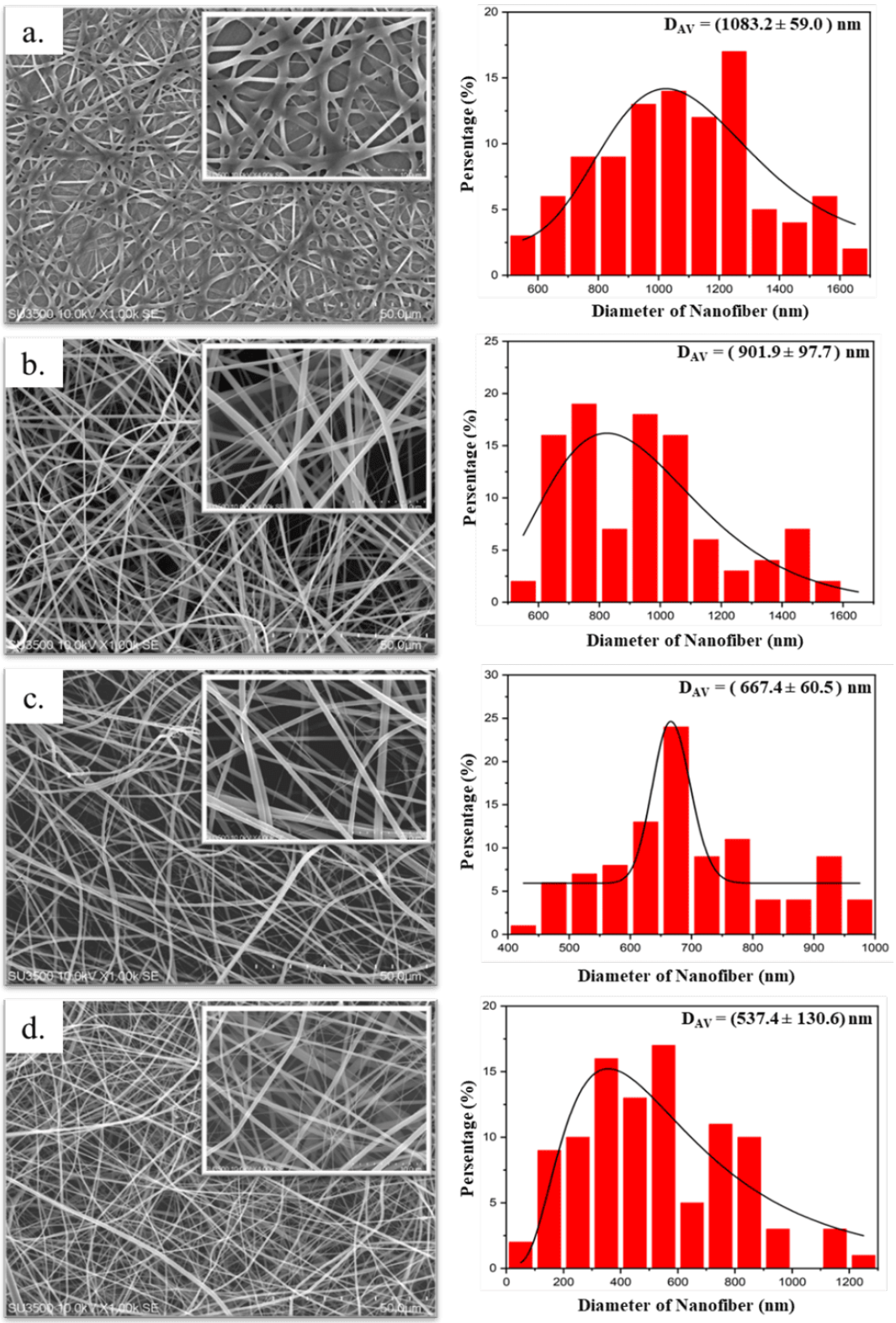

Figure 2. SEM images of EBN/PVP nanofibers and their corresponding diameter distributions at various voltages of (a) 10 kV, (b) 12.5 kV, (c) 15 kV and (d) 17.5 kV.

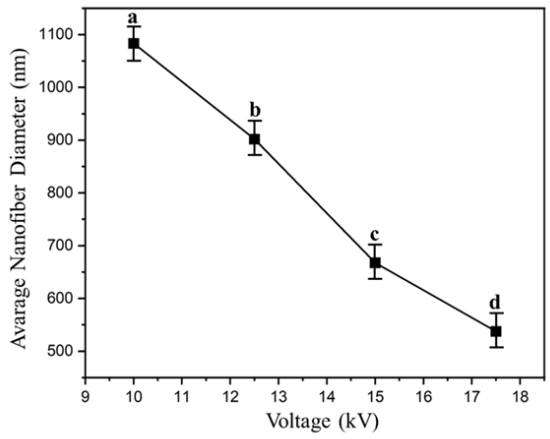

Figure 3. The effect of electrospinning operating voltage on the average diameter of EBN/PVP nanofibers. Statistical analysis was performed using Tukey's one-way ANOVA with $p < 0.05$, and alphabetical differences indicate significant differences.

Electrospinning is a versatile technique to produce nanofibers with high surface-to-volume ratios, small diameters, and excellent morphology. These unique properties make electrospun nanofibers useful in various fields such as biomedical engineering [17, 19], energy storage [20], and food packaging [21, 22].

Therefore, this study aims to investigate the optimization of electrospinning parameters for producing EBN/PVP nanofibers. Some parameters are studied, including the EBN to PVP weight ratio, electrospinning voltage, and collector distance on the diameter and morphology of the obtained fibers. Some physical characterizations were also conducted for the nanofibers, including scanning electron microscopy (SEM), Fourier transform infrared (FTIR) spectroscopy, and thermal analysis.

2. METHODS

2.1 Materials for Precursor Solution

EBN was obtained from a local market in Indonesia. Meanwhile, polyvinylpyrrolidone (PVP) with an average molecular weight of ~360,000 g/mol and absolute ethanol were obtained from Sigma-Aldrich Chemicals. The precursor solution was prepared by dissolving the PVP in ethanol to form a homogeneous solution with polymer concentration of 10 wt%. Then, EBN powder was added to the PVP solution at various EBN:PVP weight ratios of 10:90, 20:80, 30:70, 40:60, 50:50, 60:40, 70:30, 80:20, 90:10, and 100:0.

2.2 Electrospinning Process

Nanofiber were produced using an electrospinning machine (ILMI-N101 Electrospinning, Indonesia), as shown in Figure 1. The precursor solution was dispensed using a syringe pump at a constant flow rate of 0.8 mL h^{-1}. A high voltage power supply was connected to the syringe needle which will draw the solution jet toward a grounded plate collector, forming fine nanofibers. The fabrication process was conducted at a constant temperature of 26 °C and relative humidity of 55%. Some parameters were varied for the electrospinning process, including the EBN ratio in the precursor solution, working voltage, and collector distance.

2.3 Nanofiber's Characterization

The morphology and diameter of the nanofibers were analyzed using Scanning Electron Microscopy (SEM, SU3500). The diameter distribution was determined from SEM images using ImageJ software (National Institutes of Health, Bethesda, MD, USA) [23]. The functional groups of EBN/PVP nanofiber samples was investigated using Fourier Transform Infrared Spectroscopy (FTIR, Bruker, Alpha Platinum ATR A220/D-01) in wave number range of 500 to 4500 cm^{-1}. Thermal characterization was also performed to determine the thermal stability of the nanofiber samples using thermogravimetric and differential thermal analysis (TG/DTA, STA7300, Hitachi). The TG/DTA measurements were performed using the temperature range of 30 °C to 600 °C, and heating rate of 10 °C/min. The statistical analysis was also performed to the samples using Tukey's one-way ANOVA with $p < 0.05$ [24]. Minitab software version 17 (Minitab, LLC, State College, PA, USA) was used for this statistical analysis.

3. RESULTS AND DISCUSSION

3.1 Spinnability of Precursor Solution with Various EBN/PVP Ratio

To evaluate the spinnability of the precursor solutions, various weight ratios of EBN to PVP were prepared. The precursor solutions were prepared with various EBN:PVP weight ratios of 10:90, 20:80, 30:70, 40:60, 50:50, 60:40, 70:30, 80:20, 90:10, 100:0. Each solution was processed at a constant voltage of 15 kV, a fixed collector distance of 20 cm, and a constant flow rate of 0.8 mL h^{-1}. The results indicate that smooth, beads free nanofibers were successfully produced from solutions with EBN:PVP ratio of 10:90, to 60:40. The smooth morphology of nanofibers can be obtained by careful selection of the EBN/PVP ratio. It is likely that the ratio between 10:90 and 60:40 provide a favorable balance of the solution conductivity and viscosity for successful electrospinning, resulting in the formation of uniform, defect-free nanofibers.

In contrast, nanofibers were not formed for the EBN:PVP ratio of 70:30, 80:20, 90:10, 100:0. This suggests that EBN alone lacks sufficient electrospinnability and must be blended with polymeric additives such as PVP. The inability to form fibers at higher EBN content may be attributed to excessive solution viscosity, which impedes the electrospinning process [10]. Since maximizing the functional benefits of EBN is essential, nanofiber samples with the highest EBN content were selected for further optimization of electrospinning process parameters. Accordingly, the EBN:PVP ratio of 60:40 was chosen as the precursor formulation for subsequent optimization studies.

3.2 Effect of Process Parameters on the Nanofibers Diameter

The diameter of nanofibers produced by electrospinning is highly dependent on the electrospinning voltage. Figure 2 shows the morphology and diameter distribution of EBN/PVP nanofibers (EBN:PVP ratio of 60:40) obtained from various electrospinning voltages at constant solution flow rate of 0.8 mL h^{-1}, and a needle-to-collector distance of 20 cm. Generally, as the voltage increases, the average diameter of the nanofiber decreases as indicated by Figure 3. Statistical analysis using Tukey's test, represented by different alphabetical groupings, further confirms the significant differences in fiber diameters obtained at varying electrospinning voltages.

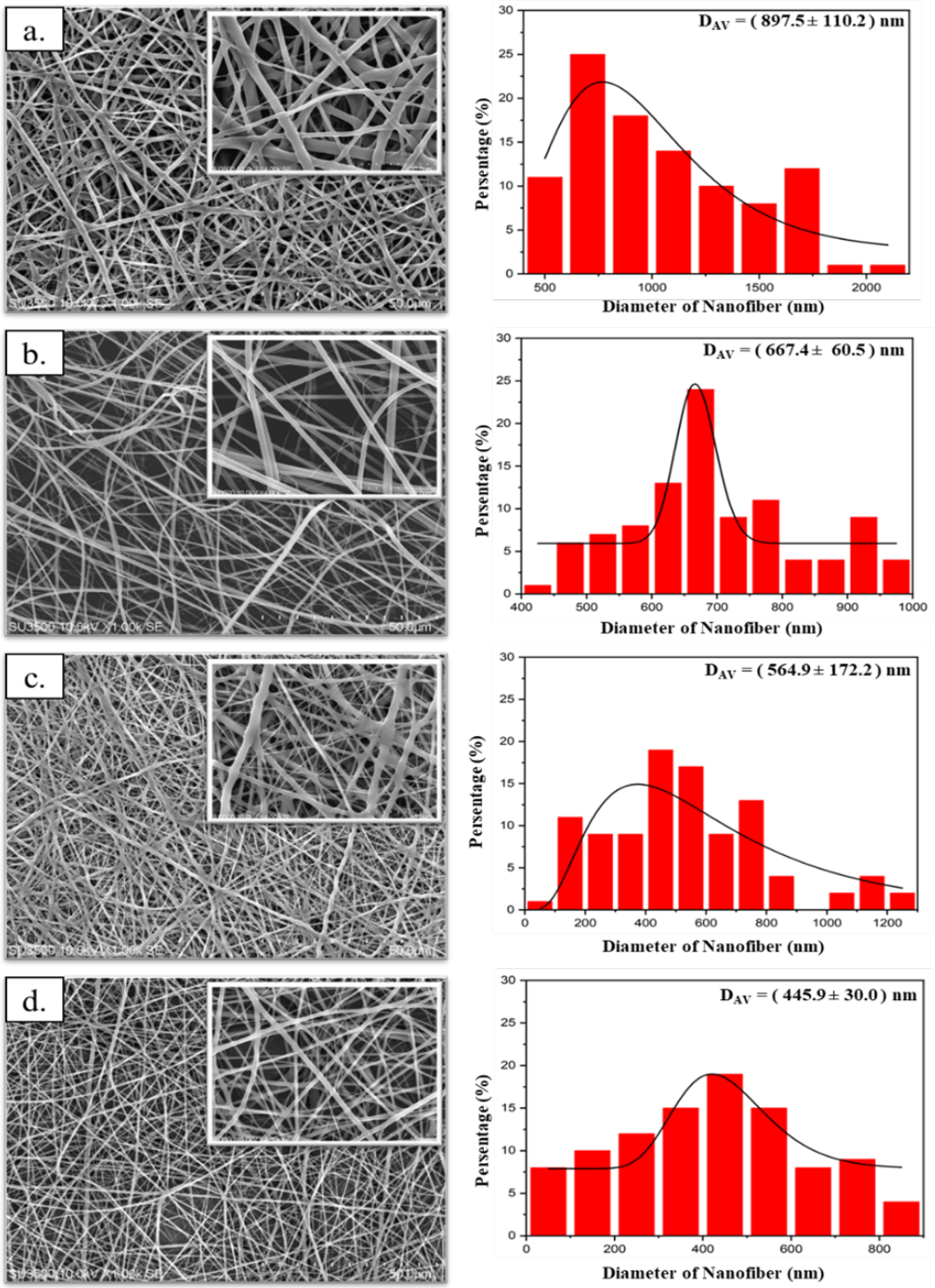

Figure 4. SEM images of EBN/PVP nanofibers and their corresponding diameter distributions fabricated using various collector distances of (a) 18 cm, (b) 20 cm, (c) 22 cm, (d) 24 cm.

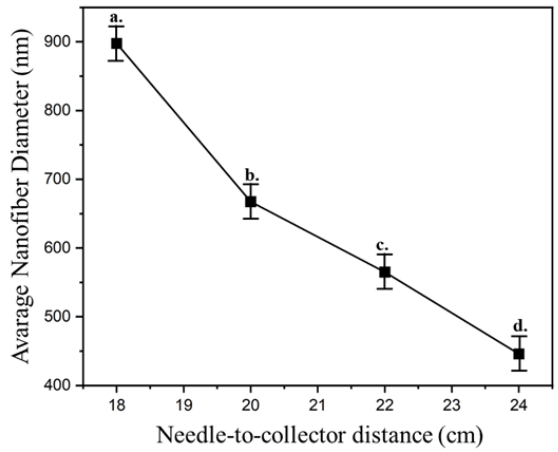

Figure 5. Effect of collector distance on the average diameter of EBN/PVP nanofibers. Statistical analysis was performed using Tukey's one-way ANOVA with $p < 0.05$, and alphabetical differences indicate significant differences.

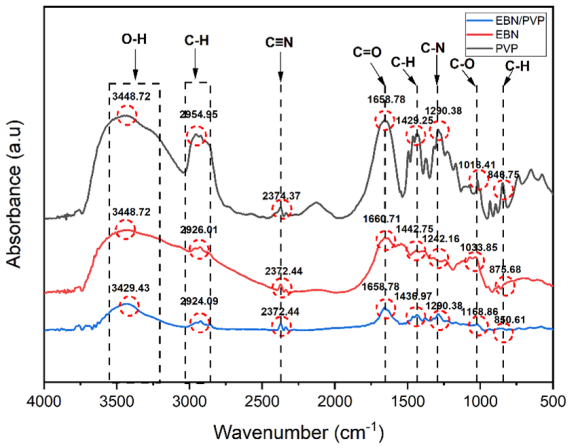

Figure 6. FTIR plots for EBN, PVP, and EBN/PVP (60:40) samples.

These results are consistent with previous studies on electrospinning of biopolymers at different voltages [25, 26]. The decrease of nanofiber diameter with increasing voltage can be attributed to the increase of electric force acting on the polymer solution during electrospinning [27, 28, 29]. This force causes the solution jet to stretch and form whipping mode before reaching collector [30]. Stronger electrostatic forces cause greater stretching on the polymer jet, resulting in a more reduction in nanofiber diameter [31, 32].

These results indicate that proper control of the electrospinning voltage is essential to produce EBN/PVP nanofibers with the desired diameter. While higher voltage may result in smaller diameter nanofibers, it may also increase the possibility of beads formation and fiber discontinuity. Therefore, the optimal electrospinning voltage should be carefully selected based on the desired nanofiber morphology and diameter.

In addition to the voltage, the distance between the needle and the collector affects the size of the EBN/PVP nanofiber produced during the electrospinning process. Figure 4 shows the effect of varying distance of the collector on the diameter distribution of the EBN/PVP nanofiber. The experiment used fixed voltage of 15 kV and solution flow rate of 0.8 mL h^{-1} for EBN:PVP ratio of 60:40. Figure 5 shows that the larger the distance between the needle and collector during electrospinning, the smaller the average diameter of the nanofiber. This is in agreement with research conducted by Z AL-Hazeem, (2020), which shows that by increasing the distance between the needle and the collector, a smaller fiber diameter and a more uniform size distribution can be obtained [33].

A shorter needle-to-collector distance can lead to larger fiber diameters, as the jet has less time to undergo full elongation during the stretching process [33]. The jet may reach the collector before sufficient stretching occurs, resulting in thicker fibers. Additionally, the reduced distance may prevent complete solvent evaporation, causing the fibers to remain wet upon deposition and potentially leading to fused fibers. Fused fibers often appear flattened and may resemble very large fibers in SEM images, potentially leading to misinterpretation of fiber diameter. In this case, the SEM image on Figure 4(a) indicates the fused fiber morphology with large fiber diameter.

3.3 FTIR Analysis

The FTIR spectra of PVP, EBN, and EBN/PVP nanofibers are presented in Figure 6. The FTIR spectrum of EBN displays several characteristic peaks that reflect its complex chemical composition [34]. The presence of proteins, particularly glycoproteins and sialoproteins, is indicated by the appearance of amide I and II bands, as well as broad O-H and N-H stretching vibrations. Carbohydrate components, such as sialic acid, are associated with pronounced C-O stretching peaks [35]. A broad peak at 3448.72 cm^{-1} corresponds to hydroxyl groups (O-H), which may be attributed to moisture content and the hydrophilic nature of protein constituents like sialoproteins and glycoproteins [36, 37, 38]. The absorption band at 2926.01 cm^{-1} represents aliphatic C–H stretching, commonly associated with the carbon chains of amino acids and lipids [35, 38, 34]. The peak at 2372.44 cm^{-1} indicates the presence of a triple bond between carbon and nitrogen (C≡N). A peak at 1242.16 cm^{-1} is attributed to the stretching of carbon–nitrogen triple bonds (C≡N). Peaks at 1242.16 cm^{-1} and 1660.71 cm^{-1} are indicative of C–N and C=O functional groups, which are fundamental to protein and amino acid structures. The band at 1242.16 cm^{-1} also reflects C–O stretching associated with carbohydrate residues such as sialic acid and glucosamine found in EBN [39, 40, 41, 42, 43, 44].

The FTIR spectrum of PVP reveals several well-defined peaks corresponding to its polymeric structure [45, 46, 47]. A strong absorption at 1658.78 cm^{-1} represents the C=O stretching of the amide group, characteristic of the pyrrolidone ring in PVP [44, 47, 48]. The band at 3429.43 cm^{-1} indicates the presence of hydroxyl (O–H) groups, a reflection of PVP's hydrophilic nature [47, 49]. The peak at 2924.09 cm^{-1} corresponds to aliphatic C–H stretching, while the peak at 2372.44 cm^{-1} indicates the presence of (C≡N) triple bonds. The absorption at 1436.97 cm^{-1} is associated with C–N stretching, confirming the presence of amide linkages within the polymer backbone [47, 50]. Additionally, a peak at 1033.85 cm^{-1} suggests the presence of C–O bonds, consistent with ether groups in the polymer structure [12, 47].

The FTIR spectrum of the EBN/PVP nanofibers displays a combination of characteristic features from both EBN and PVP, indicating successful blending of the two components. A broad peak corresponding to O–H stretching is observed, which may originate from moisture, hydroxyl groups in EBN,

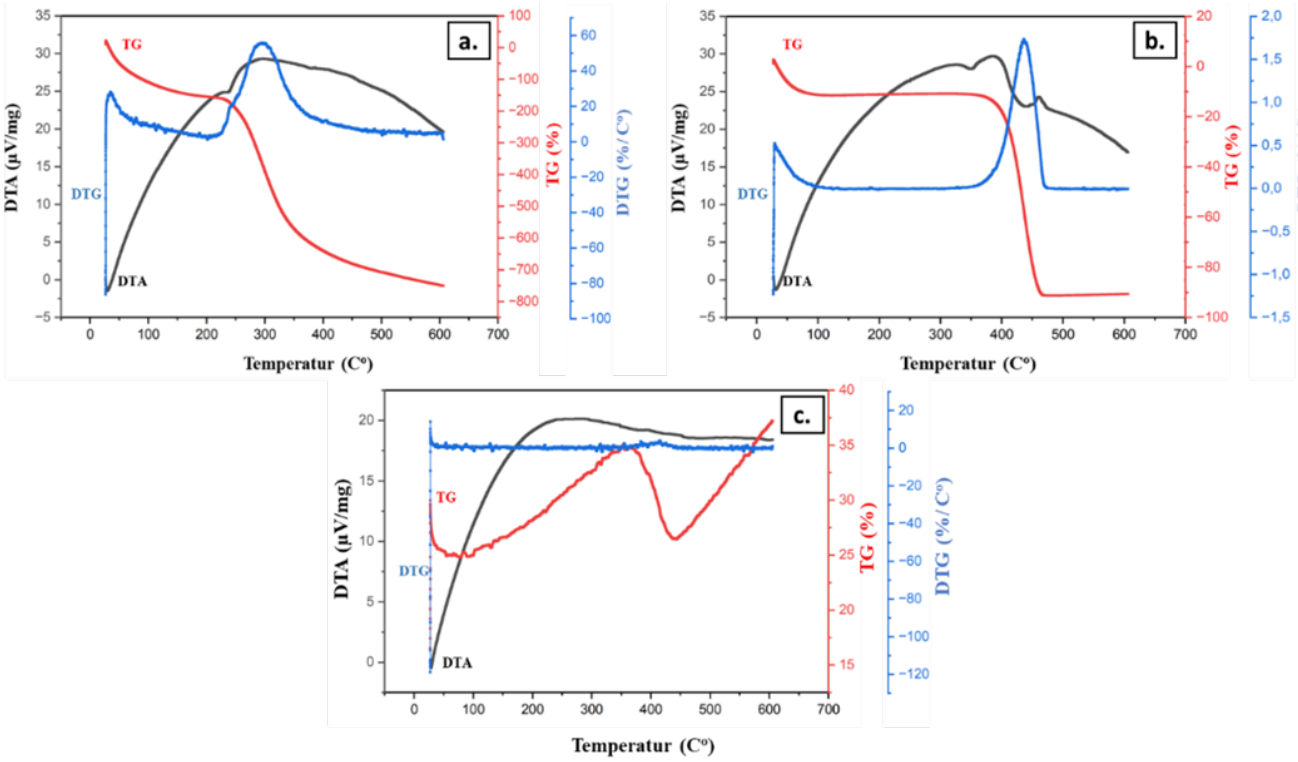

Figure 7. Thermal graphs of TG, DTG, and DTA for (a) pure EBN, (b) PVP powder, and (c) EBN/PVP nanofiber.

or hydrogen bonding between EBN and PVP. The C=O stretching band confirms the presence of carbonyl groups derived from both the amide bonds in PVP and the protein content of EBN. A peak at 2954.95 cm^{-1} is attributed to aliphatic C–H bonds, indicative of PVP's carbon backbone. Furthermore, the absorption bands at 1442.75 cm^{-1} and 1242.16 cm^{-1} correspond to C–N and C–O stretching, respectively, reflecting the amide and ether structures contributed by PVP and the carbohydrate content of EBN [46, 51].

3.4 Thermal Analysis

Thermal analysis was performed on EBN powder, PVP powder, and electrospun EBN/PVP composite nanofibers to evaluate their thermal stability and decomposition behavior. The results are presented as thermogravimetric (TG), derivative thermogravimetric (DTG), and differential thermal analysis (DTA) curves, which collectively provide insights into mass loss, decomposition kinetics, and associated enthalpy changes during thermal degradation [52, 53]. Figure 7 illustrates the thermal profiles of pure EBN, pure PVP, and the EBN/PVP nanofibers, enabling direct comparison of their thermal performance.

Figure 7(a) presents the TG curve of EBN powder. A substantial weight loss is observed in the temperature range of approximately 250°C to 500°C, indicating the thermal decomposition of organic constituents [54, 55, 56, 57]. The corresponding DTG curve exhibits a prominent peak at around 295°C, representing the temperature at which the maximum rate of decomposition occurs. Additionally, the DTA curve reveals an endothermic peak, suggesting a decomposition process or a possible phase transition. These findings indicate that EBN powder is relatively susceptible to thermal degradation at moderate temperatures.

Figure 7(b) illustrates the thermal behavior of pure PVP powder. The TG curve demonstrates that PVP exhibits superior thermal stability, with significant weight loss initiating only above 400°C. A prominent DTG peak is observed at approximately 435°C, indicating the temperature at which the maximum decomposition rate occurs [58]. The DTA curve also displays an endothermic peak corresponding to the decomposition process. These results confirm that PVP possesses high thermal stability and is capable of withstanding elevated temperatures without substantial degradation [59, 60].

Figure 7(c) shows the TG curve of the electrospun EBN/PVP nanofiber composite, revealing two distinct phases of weight loss: the first occurring between 200°C and 350°C, and the second above 450°C [61, 62]. The corresponding DTG peaks within these ranges indicate a two-step decomposition process, which can be attributed to the sequential degradation of EBN and PVP components, respectively. The DTA curve also displays two endothermic peaks, supporting the occurrence of gradual thermal transitions resulting from the composite nature of the material. These findings suggest that, although each component retains its inherent thermal behavior, the EBN/PVP nanofibers exhibit enhanced thermal stability compared to pure EBN, likely due to the stabilizing effect of the PVP matrix [63, 64, 65].

4. CONCLUSION

The electrospun EBN/PVP nanofibers were successfully synthesized. Smooth, homogeneous, and defect-free fibers were obtained from precursor solutions with EBN/PVP ratios ranging from 10:90 to 60:40. The fiber diameter decreased with increasing electrospinning voltage and collector distance. FTIR analysis confirmed the successful synthesis of EBN/PVP nanofibers by displaying characteristic peaks from both pure PVP and EBN. Thermal analysis indicated enhanced ther-

mal stability of EBN/PVP nanofibers compared to pure EBN. Owing to their favorable morphology, stability, and biocompatibility, these nanofibers hold promising potential for future applications in functional food delivery systems, nutraceutical encapsulation, or biomedical fields where controlled release and protection of bioactive compounds are essential.

DATA AVAILABILITY STATEMENT

The datasets generated during and/or analyzed during the current study are available from the corresponding author on reasonable request.

CONFLICT OF INTEREST

The authors declare that there are no conflicts of interest.

REFERENCES

[1] D. Sri Wahyuni, ULASAN SARANG BURUNG WALET SEBAGAI PANGAN FUNGSIONAL, Acta VETERINARIA Indonesiana 9 (3) (2021) 201–214. https://doi.org/10.29244/avi.9.3.201-214.

[2] T. H. Lee, W. A. Wani, C. H. Lee, K. K. Cheng, S. Shreaz, S. Wong, N. Hamdan, N. A. Azmi, Edible Bird's Nest: The Functional Values of the Prized Animal-Based Bioproduct From Southeast Asia–A Review, Frontiers in Pharmacology 12 (2021) 626233. https://doi.org/10.3389/fphar.2021.626233.

[3] Q. W. S. Lai, M. S. S. Guo, K. Q. Wu, Z. Liao, D. Guan, T. T. Dong, P. Tong, K. W. K. Tsim, Edible Bird's Nest, an Asian Health Food Supplement, Possesses Moisturizing Effect by Regulating Expression of Filaggrin in Skin Keratinocyte, Frontiers in Pharmacology 12 (2021) 685982. https://doi.org/10.3389/fphar.2021.685982.

[4] I. Fatmawati S, Haeruddin, W. O. Mulyana, Uji Aktivitas Antioksidan Ekstrak Etil Asetat Daun Belimbing Wuluh (Aveerrhoa bilimbi L.) dengan Metode DPPH, Sains: Jurnal Kimia dan Pendidikan Kimia 12 (1) (2023) 41–49. https://doi.org/10.36709/sains.v12i1.31.

[5] N. Daud, S. Mohamad Yusop, A. S. Babji, S. J. Lim, S. R. Sarbini, T. Hui Yan, Edible Bird's Nest: Physicochemical Properties, Production, and Application of Bioactive Extracts and Glycopeptides, Food Reviews International 37 (2) (2021) 177–196. https://doi.org/10.1080/87559129.2019.1696359.

[6] M. C. Quek, N. L. Chin, Y. A. Yusof, C. L. Law, S. W. Tan, Characterization of edible bird's nest of different production, species and geographical origins using nutritional composition, physicochemical properties and antioxidant activities, Food Research International 109 (2018) 35–43. https://doi.org/10.1016/j.foodres.2018.03.078.

[7] Z. Hamzah, N. H. Ibrahim, NUTRITIONAL PROPERTIES OF EDIBLE BIRD NEST, Journal of Asian Scientific Research (2013).

[8] Evaluation of Nitrite Concentration in Edible Bird's Nest (White, Yellow, Orange, and Red Blood), Makara Journal of Science 26 (1) (Mar. 2022). https://doi.org/10.7454/mss.v26i1.1311.

[9] X. Liu, X. Song, D. Gou, H. Li, L. Jiang, M. Yuan, M. Yuan, A polylactide based multifunctional hydrophobic film for tracking evaluation and maintaining beef freshness by an electrospinning technique, Food Chemistry 428 (2023) 136784. https://doi.org/10.1016/j.foodchem.2023.136784.

[10] Y. A. Rezeki, D. Harjunowibowo, P. Indrayudha, M. Alauhdin, I. K. Fitri, L. D. Setyaningsih, F. Udaneni, ELECTROSPINNING DAN ELECTROSPRAY: TEKNIK PABRIKASI NANOFIBER DAN NANOPARTIKEL.

[11] M. Ali, S. Mir, L. I. Atanase, O.-U.-R. Abid, M. Kazi, Chitosan–PVA–PVP/nano-clay composite: a promising tool for controlled drug delivery, RSC Advances 14 (22) (2024) 15777–15790. https://doi.org/10.1039/D4RA02959C.

[12] I. Sriyanti, D. Edikresnha, M. M. Munir, H. Rachmawati, Khairurrijal, Electrospun Polyvinylpyrrolidone (PVP) Nanofiber Mats Loaded by *Garcinia mangostana* L. Extracts, Materials Science Forum 880 (2016) 11–14. https://doi.org/10.4028/www.scientific.net/MSF.880.11.

[13] A. Priyanto, D. A. Hapidin, T. Suciati, K. Khairurrijal, Current Developments on Rotary Forcespun Nanofibers and Prospects for Edible Applications, Food Engineering Reviews 14 (3) (2022) 435–461. https://doi.org/10.1007/s12393-021-09304-w.

[14] S. Zhang, Fabrication of novel biomaterials through molecular self-assembly, Nature Biotechnology 21 (10) (2003) 1171–1178. https://doi.org/10.1038/nbt874.

[15] P. X. Ma, R. Zhang, Synthetic nano-scale fibrous extracellular matrix, Journal of Biomedical Materials Research 46 (1) (1999) 60–72. https://doi.org/10.1002/(SICI)1097-4636(199907)46:1<60::AID-JBM7>3.0.CO;2-H.

[16] W. Zhu, X. Ma, M. Gou, D. Mei, K. Zhang, S. Chen, 3D printing of functional biomaterials for tissue engineering, Current Opinion in Biotechnology 40 (2016) 103–112. https://doi.org/10.1016/j.copbio.2016.03.014.

[17] S. Wu, T. Dong, Y. Li, M. Sun, Y. Qi, J. Liu, M. A. Kuss, S. Chen, B. Duan, State-of-the-art review of advanced electrospun nanofiber yarn-based textiles for biomedical applications, Applied Materials Today 27 (2022) 101473. https://doi.org/10.1016/j.apmt.2022.101473.

[18] L. Nulhakim, KARAKTERISTIK NANOGENERATOR PIEZOELEKTRIK ZnO DOPING Co3O4, Simetris: Jurnal Teknik Mesin, Elektro dan Ilmu Komputer 9 (1) (2018) 687–692. https://doi.org/10.24176/simet.v9i1.1821.

[19] T. Wu, X. Mo, Y. Xia, Moving Electrospun Nanofibers and Bioprinted Scaffolds toward Translational Applications, Advanced Healthcare Materials 9 (6) (2020) 1901761. https://doi.org/10.1002/adhm.201901761.

[20] Y. Yan, X. Liu, J. Yan, C. Guan, J. Wang, Electrospun Nanofibers for New Generation Flexible Energy Storage, ENERGY & ENVIRONMENTAL MATERIALS 4 (4) (2021) 502–521. https://doi.org/10.1002/eem2.12146.

[21] S. Forghani, H. Almasi, M. Moradi, Electrospun nanofibers as food freshness and time-temperature indicators: A new approach in food intelligent packaging, Innovative Food Science & Emerging Technologies 73 (2021) 102804. https://doi.org/10.1016/j.ifset.2021.102804.

[22] F. Topuz, T. Uyar, Antioxidant, antibacterial and antifungal electrospun nanofibers for food packaging applications, Food Research International 130 (2020) 108927. https://doi.org/10.1016/j.foodres.2019.108927.

[23] C. A. Schneider, W. S. Rasband, K. W. Eliceiri, NIH Image to ImageJ: 25 years of image analysis, Nature Methods 9 (7) (2012) 671–675. https://doi.org/10.1038/nmeth.2089.

[24] Y. Chen, X. Liu, M. Yang, W. Sun, C. Mao, Integration of genetically engineered virus nanofibers and fibrin to form injectable fibrous neuron-rich hydrogels and enable neural differentiation, Journal of Materials Chemistry B 11 (4) (2023) 802–815. https://doi.org/10.1039/D2TB01712A.

[25] P. Shao, B. Niu, H. Chen, P. Sun, Fabrication and characterization of tea polyphenols loaded pullulan-CMC electrospun nanofiber for fruit preservation, International Journal of Biological Macromolecules 107 (2018) 1908–1914. https://doi.org/10.1016/j.ijbiomac.2017.10.054.

[26] A. Asiri, R. H. Al-Ashwal, M. H. Sani, S. Saidin, Effects of Electrospinning Voltage and Flow Rate on Morphology of Poly-vinyl Alcohol Nanofibers, Journal of Physics: Conference Series 1372 (1) (2019) 012035. https://doi.org/10.1088/1742-6596/1372/1/012035.

[27] H. Niragire, T. G. Kebede, S. Dube, M. Maaza, M. M. Nindi, Chitosan-based electrospun nanofibers mat for the removal of acidic drugs from influent and effluent, Chemical Engineering Communications 210 (9) (2023) 1485–1507. https://doi.org/10.1080/00986445.2022.2116321.

[28] A. G. Şener, A. S. Altay, F. Altay, Effect of voltage on morphology of electrospun nanofibers, Institute Of Electrical and Electronics Engineer, Bursa, Turkey, 2011.

[29] M. Ahmadi Bonakdar, D. Rodrigue, Electrospinning: Processes, Structures, and Materials, Macromol 4 (1) (2024) 58–103. https://doi.org/10.3390/macromol4010004.

[30] L. Zhan, J. Deng, Q. Ke, X. Li, Y. Ouyang, C. Huang, X. Liu, Y. Qian, Grooved Fibers: Preparation Principles Through Electrospinning and Potential Applications, Advanced Fiber Materials 4 (2) (2022) 203–213. https://doi.org/10.1007/s42765-021-00116-5.

[31] R. Amna, K. Ali, M. I. Malik, S. I. Shamsah, A Brief Review of Electrospinning of Polymer Nanofibers: History and Main Applications, Journal of New Materials for Electrochemical Systems 23 (3) (2020) 151–163. https://doi.org/10.14447/jnmes.v23i3.a01.

[32] N. Z Al-Hazeem, Effect of the Distance between the Needle Tip and the Collector on Nanofibers Morphology, Nanomedicine & Nanotechnology Open Access 5 (3) (2020). https://doi.org/10.23880/NNOA-16000195.

[33] C. Campanale, I. Savino, C. Massarelli, V. F. Uricchio, Fourier Transform Infrared Spectroscopy to Assess the Degree of Alteration of Artificially Aged and Environmentally Weathered Microplastics, Polymers 15 (4) (2023) 911. https://doi.org/10.3390/polym15040911.

[34] M. Yuan, X. Lin, D. Wang, J. Dai, Proteins: Neglected active ingredients in edible bird's nest, Chinese Herbal Medicines 15 (3) (2023) 383–390. https://doi.org/10.1016/j.chmed.2023.02.004.

[35] R. Mohamad Ibrahim, N. N. Mohamad Nasir, M. Z. Abu Bakar, R. Mahmud, N. A. Ab Razak, The Authentication and Grading of Edible Bird's Nest by Metabolite, Nutritional, and Mineral Profiling, Foods 10 (7) (2021) 1574. https://doi.org/10.3390/foods10071574.

[36] M. D. Ohi, EM Analysis of Protein Structure, in: Encyclopedia of Life Sciences, 1st Edition, Wiley, 2009. https://doi.org/10.1002/9780470015902.a0021885.
URL https://onlinelibrary.wiley.com/doi/10.1002/9780470015902.a0021885

[37] H. Yuan, S. Tang, Q. Luo, T. Xiao, W. Wang, Q. Ma, X. Guo, Y. Wu, Micro-FTIR spectroscopy and partial least-squares regression for rapid determination of moisture content of nanogram-scaled heat-treated wood, Journal of Wood Science 66 (1) (2020) 1. https://doi.org/10.1186/s10086-020-1848-7.

[38] J. De Meutter, E. Goormaghtigh, Amino acid side chain contribution to protein FTIR spectra: impact on secondary structure evaluation, European Biophysics Journal 50 (3-4) (2021) 641–651. https://doi.org/10.1007/s00249-021-01507-7.

[39] C. H. Lee, T. H. Lee, S. L. Wong, B. B. Nyakuma, N. Hamdan, S. C. Khoo, H. Ramachandran, H. Jamaluddin, Characteristics and trends in global Edible Bird's Nest (EBN) research (2002–2021): a review and bibliometric study, Journal of Food Measurement and Characterization 17 (5) (2023) 4905–4926. https://doi.org/10.1007/s11694-023-02006-3.

[40] L. Guo, Y. Wu, M. Liu, Y. Ge, Y. Chen, Rapid authentication of edible bird's nest by FTIR spectroscopy combined with chemometrics, Journal of the Science of Food and Agriculture 98 (8) (2018) 3057–3065. https://doi.org/10.1002/jsfa.8805.

[41] C. H. Ng, P. L. Tang, Y. Y. Ong, Enzymatic hydrolysis improves digestibility of edible bird's nest (EBN): combined effect of pretreatment and enzyme, Journal of Food Measurement and Characterization 17 (1) (2023) 549–563. https://doi.org/10.1007/s11694-022-01648-z.

[42] A. Ujuldah, A. R. Hakim, R. Saputri, FTIR Spectroscopic Characterization of Edible Bird's Nest From Jenamas Central Kalimantan 1 (1) (2023).

[43] J. S. Ng, S. A. Muhammad, C. H. Yong, A. Mohd Rodhi, B. Ibrahim, M. N. H. Adenan, S. Moosa, Z. Othman, N. A. Abdullah Salim, Z. Sharif, F. Ismail, S. D. Kelly, A. Cannavan, Adulteration Detection of Edible Bird's Nests Using Rapid Spectroscopic Techniques Coupled with Multi-Class Discriminant Analysis, Foods 11 (16) (2022) 2401. https://doi.org/10.3390/foods11162401.

[44] T. Song, J. Li, Q. Deng, Y. Gao, Preparation, Characterization, Photochromic Properties, and Mechanism of PMoA/ZnO/PVP Composite Film, Molecules 28 (22) (2023) 7605. https://doi.org/10.3390/molecules28227605.

[45] R. P. D'Amelia, S. Gentile, W. F. Nirode, L. Huang, Quantitative Analysis of Copolymers and Blends of Polyvinyl Acetate (PVAc) Using Fourier Transform Infrared Spectroscopy (FTIR) and Elemental Analysis (EA).

[46] I. A. Safo, M. Werheid, C. Dosche, M. Oezaslan, The role of polyvinylpyrrolidone (PVP) as a capping and structure-directing agent in the formation of Pt nanocubes, Nanoscale Advances 1 (8) (2019) 3095–3106. https://doi.org/10.1039/C9NA00186G.

[47] P. C. V. I. A, Transformação De Plastômeros.

[48] N. Roy, N. Saha, PVP-based hydrogels: Synthesis, properties and applications (May 2016).

[49] V. E. Zhivulin, R. K. Khairanov, N. A. Zlobina, L. A. Pesin, Modification of the IR Spectra Shape in the 2000–2300 cm–1 Absorption Band upon the Aging of a Chemically Dehydrofluorinated Poly(vinylidene fluoride) Film, Journal of Surface Investigation: X-ray, Synchrotron and Neutron Techniques 14 (6) (2020) 1144–1151. https://doi.org/10.1134/S1027451020060178.

[50] A. A. Mahmoud, O. Osman, K. Eid, E. A. Ashkar, A. Okasha, D. Atta, M. Eid, Z. A. Aziz, A. Fakhry, FTIR Spectroscopy of Natural Bio-Polymers Blends (2014).

[51] Y. Lv, F. Xu, F. Liu, M. Chen, Investigation of Structural Characteristics and Solubility Mechanism of Edible Bird Nest: A Mucin Glycoprotein, Foods 12 (4) (2023) 688. https://doi.org/10.3390/foods12040688.

[52] M. Feist, Thermal analysis: basics, applications, and benefit, ChemTexts 1 (1) (2015) 8. https://doi.org/10.1007/s40828-015-0008-y.

[53] F. Rashid, M. Al-Obaidi, A. Dulaimi, L. Bernardo, M. Eleiwi, H. Mahood, A. Hashim, A Review of Recent Improvements, Developments, Effects, and Challenges on Using Phase-Change Materials in Concrete for Thermal Energy Storage and Release, Journal of Composites Science 7 (9) (2023) 352. https://doi.org/10.3390/jcs7090352.

[54] E. Díaz-Montes, Polysaccharides: Sources, Characteristics, Properties, and Their Application in Biodegradable Films, Polysaccharides 3 (3) (2022) 480–501. https://doi.org/10.3390/polysaccharides3030029.

[55] H. L. Ornaghi, M. Faccio, M. R. F. Soares, Thermal Degradation Kinetics of Natural Fibers: Determination of the Kinetic Triplet and Lifetime Prediction, Polysaccharides 5 (3) (2024) 169–183. https://doi.org/10.3390/polysaccharides5030013.

[56] X. Qi, Y. Zhang, H. Yu, J. Xie, Research on the Properties of Polysaccharides, Starch, Protein, Pectin, and Fibre in Food Processing, Foods 12 (2) (2023) 249. https://doi.org/10.3390/foods12020249.

[57] M. S. Saracoglu, M. K. Coruh, Thermal degradation properties, kinetic, thermodynamic and reaction mechanism of pyrolysis of biomass shells: pistachio, almond, walnut and hazelnut as bioenergy potential, Biomass Conversion and Biorefinery 14 (24) (2024) 32427–32452. https://doi.org/10.1007/s13399-023-05052-5.

[58] B. Krause, S. Imhoff, B. Voit, P. Pötschke, Influence of Polyvinylpyrrolidone on Thermoelectric Properties of Melt-Mixed Polymer/Carbon Nanotube Composites, Micromachines 14 (1) (2023) 181. https://doi.org/10.3390/mi14010181.

[59] C. Leyva-Porras, P. Cruz-Alcantar, V. Espinosa-Solís, E. Martínez-Guerra, C. I. Piñón-Balderrama, I. Compean Martínez, M. Z. Saavedra-Leos, Application of Differential Scanning Calorimetry (DSC) and Modulated Differential Scanning Calorimetry (MDSC) in Food and Drug Industries, Polymers 12 (1) (2019) 5. https://doi.org/10.3390/polym12010005.

[60] M. I. Loría-Bastarrachea, W. Herrera-Kao, J. V. Cauich-Rodríguez, J. M. Cervantes-Uc, H. Vázquez-Torres, A. Ávila Ortega, A TG/FTIR study on the thermal degradation of

poly(vinyl pyrrolidone), Journal of Thermal Analysis and Calorimetry 104 (2) (2011) 737–742. https://doi.org/10.1007/s10973-010-1061-9.

[61] L. C. Mendes, R. C. Rodrigues, E. P. Silva, Thermal, structural and morphological assessment of PVP/HA composites, Journal of Thermal Analysis and Calorimetry 101 (3) (2010) 899–905. https://doi.org/10.1007/s10973-010-0835-4.

[62] M. A. Bkkar, R. O. Olekhnovich, A. V. Kremleva, Y. N. Kovach, V. Kalanchina, M. V. Uspenskaya, Fabrication of electrospun polymer nanofibers modified with all-inorganic perovskite nanocrystals for flexible optoelectronic devices, Applied Nanoscience 12 (10) (2022) 2961–2977. https://doi.org/10.1007/s13204-022-02603-6.

[63] J. R. P. Forgie, F. Leclinche, E. Dréan, P. I. Dolez, Electrospinning of High-Performance Nanofibres: State of the Art and Insights into the Path Forward, Applied Sciences 13 (22) (2023) 12476. https://doi.org/10.3390/app132212476.

[64] N. Palani, P. Vijayakumar, P. Monisha, S. Ayyadurai, S. Rajadesingu, Electrospun nanofibers synthesized from polymers incorporated with bioactive compounds for wound healing, Journal of Nanobiotechnology 22 (1) (2024) 211. https://doi.org/10.1186/s12951-024-02491-8.

[65] M. Tahir, S. Vicini, A. Sionkowska, Electrospun Materials Based on Polymer and Biopolymer Blends—A Review, Polymers 15 (7) (2023) 1654. https://doi.org/10.3390/polym15071654.

